

# Functionalization of Polyoxometalates: From Lindqvist to Keggin Derivatives. 1. Synthesis, Solution Studies, and Spectroscopic and ESI Mass Spectrometry Characterization of the Rhenium Phenylimido Tungstophosphate $[PW_{11}O_{39}\{ReNC_6H_5\}]^{4-}$

Céline Dablemont,<sup>†</sup> Anna Proust,<sup>\*,†</sup> René Thouvenot,<sup>†</sup> Carlos Afonso,<sup>†</sup> Françoise Fournier,<sup>†</sup> and Jean-Claude Tabet<sup>\*,†</sup>

Laboratoire de Chimie Inorganique et Matériaux Moléculaires, UMR CNRS 7071, Université Pierre et Marie Curie, 4 Place Jussieu, 75252 Paris Cedex 05, France, and Laboratoire Structure et Fonction des Molécules Bioactives, UMR CNRS 7613, Université Pierre et Marie Curie, 4 Place Jussieu, 75252 Paris Cedex 05, France

Received January 23, 2004

Reaction of  $[Bu_4N]_4[H_3PW_{11}O_{39}]$  with  $[Re(NPh)Cl_3(PPh_3)_2]$ , in acetonitrile and in the presence of  $NEt_3$ , provided the first Keggin-type organoimido derivative  $[Bu_4N]_4[PW_{11}O_{39}\{ReNPh\}]$  (Ph =  $C_6H_5$ ) (1). The functionalization was clearly demonstrated by various techniques including  $^1H$  and  $^{14}N$  NMR, electrochemistry, and ESI mass spectrometry. Conditions for the formation of 1 are also discussed.

## Introduction

Early transition metal oxygen cluster anions, or polyoxometalates (POMs), are remarkable for their molecular and electronic structural diversity<sup>1</sup> and receive considerable current interest because of their wide range of properties and their significant applications<sup>2</sup> in many fields such as analytical chemistry, catalysis, materials science, and medicine. As far as we are concerned, we have now a long tradition in the functionalization of POMs and we have been especially interested in the introduction of multiply bonded nitrogenous ligands for the synthesis of stable systems. We have thus described nitrosyl,<sup>3</sup> organoimido<sup>4</sup> and organodiazenido<sup>5</sup> derivatives related to the Lindqvist anion  $[Mo_6O_{19}]^{2-}$ . The

aryl group in  $[Mo_5O_{18}\{MoNAr\}]^{2-}$  or  $[Mo_5O_{18}\{MoN_2Ar\}]^{3-}$  allows considerable variation and this has been exploited (i) to tune the electronic properties of the hexamolybdate anion by varying the releasing or withdrawing character of the substituent and (ii) to introduce new functional groups, such as a polymerizable function<sup>6</sup> or a ferrocene unit,<sup>7</sup> as a first step in the design of POM-based molecular materials. Polyimido species,<sup>8</sup>  $[Mo_{6-x}O_{19-x}\{MoNAr\}_x]^{2-}$  with  $x$  up to 6, and several examples of interconnected hexamolybdates through bis(imido) ligands<sup>9</sup> have also been reported. As the

\* Authors to whom correspondence should be addressed. E-mail: proust@ccr.jussieu.fr (A.P.); tabet@ccr.jussieu.fr (J.-C.T.). Fax: (+33)1 44 27 38 41 (A.P.); (+33)1 44 27 38 53 (J.-C.T.).

<sup>†</sup> Laboratoire de Chimie Inorganique et Matériaux Moléculaires.

<sup>‡</sup> Laboratoire Structure et Fonction des Molécules Bioactives.

- (1) (a) Pope, M. T. *Heteropoly and Isopoly Oxometalates*; Springer-Verlag: Berlin 1983. (b) Pope, M. T.; Müller, A. *Angew. Chem., Int. Ed. Engl.* **1991**, *30*, 34–48.
- (2) (a) *Polyoxometalates: from Platonic Solids to Anti-Retroviral Activity*; Pope, M. T., Müller, A., Eds; Kluwer Academic Publishers: Dordrecht, The Netherlands, 1994. (b) *Polyoxometalates From Topology via Self-Assembly to Applications*; Pope, M. T., Müller, A., Eds; Kluwer Academic Publishers: Dordrecht, The Netherlands, 2001. (c) *Chem. Rev.* **1998**, *98*, special issue on polyoxometalates (Hill, C. L., Ed.).
- (3) (a) Proust, A.; Thouvenot, R.; Robert, F.; Gouzerh, P. *Inorg. Chem.* **1993**, *32*, 5299–5304. (b) Proust, A.; Thouvenot, R.; Roh, S.-G.; Yoo, J.-K.; Gouzerh, P. *Inorg. Chem.* **1995**, *34*, 4106–4112.

- (4) (a) Proust, A.; Thouvenot, R.; Chaussade, M.; Robert, F.; Gouzerh, P. *Inorg. Chim. Acta* **1994**, *224*, 81–95. (b) Proust, A.; Villanneau R. In ref 2b, p 23.
- (5) Bustos, C.; Hasenknopf, B.; Thouvenot, R.; Vaissermann, J.; Proust, A.; Gouzerh, P. *Eur. J. Inorg. Chem.* **2003**, 2757–2766.
- (6) Moore, A. A.; Kwen, H.; Beatty, A. M.; Maatta, E. A. *Chem. Commun.* **2000**, 1793–1794.
- (7) Stark, J. L.; Young, V. G., Jr.; Maatta, E. A. *Angew. Chem., Int. Ed. Engl.* **1995**, *34*, 2547–2548.
- (8) (a) Strong, J. B.; Ostrander, R.; Rheingold, A. L.; Maatta, E. A. *J. Am. Chem. Soc.* **1994**, *116*, 3601–3602. (b) Strong, J. B.; Yap, G. P. A.; Ostrander, R.; Liable-Sands, L. M.; Rheingold, A. L.; Thouvenot, R.; Gouzerh, P.; Maatta, E. A. *J. Am. Chem. Soc.* **2000**, *122*, 639–649.
- (9) (a) Clegg, W.; Errington, R. J.; Fraser, K.; Holmes, S. A.; Schäfer, A. *J. Chem. Soc., Chem. Commun.* **1995**, 455–456. (b) Stark, J. L.; Rheingold, A. L.; Maatta, E. A. *J. Chem. Soc., Chem. Commun.* **1995**, 1165–1166. (c) Lu, M.; Wei, Y.; Xu, B.; Cheung, C. F.-C.; Peng, Z.; Powell, D. R. *Angew. Chem., Int. Ed.* **2002**, *41*, 1566–1568. (d) Peng, Z. *Angew. Chem., Int. Ed.* **2004**, *43*, 930–935. (e) Roesner, R. A.; McGrath, S. C.; Brockman, J. T.; Moll, J. D.; West, D. X.; Swearingen, J. K.; Castineiras, A. *Inorg. Chim. Acta* **2003**, *342*, 37–47.

potential of Keggin or Dawson POM-based molecular materials should be greater than that of Lindqvist derivatives, we have now focused our attention on the functionalization of Keggin POMs. Two strategies could be considered: (i) the reaction of a suitable reagent, such as an isocyanate, a phosphinimine, or an amine, on  $[\text{PMo}_{12}\text{O}_{40}]^{3-10}$  or  $[\text{PW}_{12-x}\text{O}_{40-x}\{\text{MO}\}_x]^{3-}$ , where MO represents a reactive oxo-metal function; (ii) the reaction between a monovacant Keggin polyanion, such as  $[\text{PW}_{11}\text{O}_{39}]^{7-}$ , and a mononuclear compound containing the target metal-imido function, a procedure which proved successful for the synthesis of Keggin nitrido derivatives.<sup>11</sup> Both routes have been explored in the search for Keggin imido derivatives. In a subsequent paper, we will show that the first one is systematically hindered by the reduction of the parent polyanion. However we could obtain  $[\text{Bu}_4\text{N}]_4[\text{PW}_{11}\text{O}_{39}\{\text{ReNPh}\}]$  ( $\text{Ph} = \text{C}_6\text{H}_5$ ) by reaction of  $[\text{Bu}_4\text{N}]_4[\text{H}_3\text{PW}_{11}\text{O}_{39}]$  with  $[\text{Re}(\text{NPh})\text{Cl}_3(\text{PPh}_3)_2]$  in acetonitrile. To the best of our knowledge, this is the first example of a Keggin-type organoimido derivative. This complex has been characterized by  $^1\text{H}$  and  $^{14}\text{N}$  NMR, IR, electrochemistry, and ESI-MS (electrospray ionization mass spectrometry), which appears to be particularly well adapted to the characterization of functionalized POMs and thus deserves special attention.

## Experimental Section

**Materials.** The lacunary  $[\text{Bu}_4\text{N}]_4[\text{H}_3\text{PW}_{11}\text{O}_{39}]^{12}$  and compounds  $[\text{ReOCl}_3(\text{PPh}_3)_2]^{13}$  and  $[\text{Re}(\text{NPh})\text{Cl}_3(\text{PPh}_3)_2]^{14}$  were prepared as described in the literature but substituting toluene for benzene in the synthesis of  $[\text{Re}(\text{NPh})\text{Cl}_3(\text{PPh}_3)_2]$ . Tetrabutylammonium tetrafluoroborate was synthesized from commercial (Aldrich) sodium tetrafluoroborate and tetrabutylammonium hydrogensulfate and dried overnight at 60 °C under vacuum. Triethylamine was purchased from Aldrich and stored on sodium wire. Reagent grade acetonitrile was dried over calcium hydride before distillation. Reagent grade diethyl ether was used as received. LiOMe was prepared by reaction between metallic lithium and distilled methanol, under nitrogen. After filtration of the  $\text{Li}_2\text{O}$  eventually formed, solid LiOMe was recovered from the solution by evaporation to dryness.

**Preparation of  $[\text{Bu}_4\text{N}]_4[\text{PW}_{11}\text{O}_{39}\{\text{Re}^{\text{V}}\text{NPh}\}]$  (1).** To a solution of  $[\text{Bu}_4\text{N}]_4[\text{H}_3\text{PW}_{11}\text{O}_{39}]$  (0.365 g, 0.100 mmol) in distilled  $\text{CH}_3\text{CN}$  (10 mL) were added successively  $\text{Et}_3\text{N}$  (0.040 mL, 0.300 mmol) and  $[\text{Re}(\text{NPh})\text{Cl}_3(\text{PPh}_3)_2]$  (0.091 g, 0.100 mmol). Within a few minutes under reflux, the initially green suspension turned to a violet solution which was further refluxed for 1 h and filtered. Deep violet crystals were grown by slow diffusion of  $\text{Et}_2\text{O}$  into the filtrate (0.356 g). These crystals were found to be a mixture of  $[\text{Bu}_4\text{N}]_4[\text{PW}_{11}\text{O}_{39}\{\text{Re}^{\text{V}}\text{NPh}\}]$  (1) and  $[\text{Bu}_4\text{N}]_4[\text{PW}_{11}\text{O}_{39}\{\text{Re}^{\text{V}}\text{O}\}]$  (2). To remove any  $\text{PPh}_3$  and  $\text{Ph}_3\text{PO}$ , the crystals were washed with  $\text{Et}_2\text{O}$ .

The only way to get rid of colorless  $\text{Et}_3\text{NHCl}$  crystals was to separate them mechanically. IR (KBr):  $\nu = 2962$  (m), 2936 (m), 2874 (m), 1482 (m), 1380 (w), 1153 (w), 1077 (m), 1045 (w), 1032 (w), 1004 (w), 961 (s), 883 (s), 809 (s), 771 (s), 388 (m)  $\text{cm}^{-1}$ . UV-vis ( $\text{CH}_3\text{CN}$ ):  $\lambda_1 = 728$  nm,  $\log \epsilon_1 \sim 3.1$ ;  $\lambda_2 = 532$  nm,  $\log \epsilon_2 \sim 3.5$ .  $^1\text{H}$  NMR ( $\text{CD}_3\text{CN}$ ):  $\delta = 7.59$  (m, 2H, meta), 7.51 (m, 1H, para), 7.34 (d, 2H, ortho).  $^{14}\text{N}$  NMR ( $\text{DMF}/(\text{CD}_3)_2\text{CO}$ , 7:1, v:v):  $\delta = 30$ .  $^{31}\text{P}$  NMR ( $\text{CD}_3\text{CN}$ ):  $\delta = -14.59$  ppm.

**Preparation of  $[\text{Bu}_4\text{N}]_4[\text{PW}_{11}\text{O}_{39}\{\text{Re}^{\text{V}}\text{O}\}]$  (2), Starting with  $[\text{ReOCl}_3(\text{PPh}_3)_2]$ .** To a suspension of  $[\text{Bu}_4\text{N}]_4[\text{H}_3\text{PW}_{11}\text{O}_{39}]$  (4.000 g, 1.080 mmol) and  $[\text{ReOCl}_3(\text{PPh}_3)_2]$  (0.960 g, 1.160 mmol) in distilled  $\text{CH}_3\text{CN}$  (160 mL) was added  $\text{Et}_3\text{N}$  (0.440 mL, 3.160 mmol). Within a few minutes, the initially yellow suspension turned to a violet solution, which was stirred overnight at room temperature, filtered, and half-concentrated. Deep violet crystals of  $[\text{Bu}_4\text{N}]_4[\text{PW}_{11}\text{O}_{39}\{\text{Re}^{\text{V}}\text{O}\}]$  (2) were grown by slow diffusion of  $\text{Et}_2\text{O}$  into the filtrate. Sometimes, the crystals were found to be contaminated with  $\text{Et}_3\text{NHCl}$ ,  $\text{PPh}_3$ , or  $\text{Ph}_3\text{PO}$ . Extensive washing with water and  $\text{Et}_2\text{O}$  then allowed us to remove these impurities. Yield: 3.670 g (88%). IR (KBr):  $\nu = 2962$  (m), 2936 (m), 2874 (m), 1483 (m), 1382 (m), 1382 (w), 1105 (w), 1076 (m), 1058 (sh), 963 (s), 884 (s), 811 (s), 776 (s), 389 (m)  $\text{cm}^{-1}$ .  $^{31}\text{P}$  NMR ( $\text{CD}_3\text{CN}$ ):  $\delta = -14.59$  ppm.

**Refluxing of  $[\text{Re}(\text{NPh})\text{Cl}_3(\text{PPh}_3)_2]$  in Acetonitrile.** A suspension of  $[\text{Re}(\text{NPh})\text{Cl}_3(\text{PPh}_3)_2]$  (0.045 g, 0.050 mmol) in acetonitrile (5 mL) was refluxed for 1 h. The green solid was filtered off and identified as pure  $[\text{Re}(\text{NPh})\text{Cl}_3(\text{PPh}_3)_2]$  by  $^{31}\text{P}$  NMR, and the  $^{31}\text{P}$  NMR spectrum of the filtrate was recorded in  $\text{CH}_3\text{CN}/\text{CD}_3\text{CN}$  (2:1, v:v):  $-4.55$  (39%,  $\text{PPh}_3$ ),  $-15.03$  (31%),  $-17.91$  ppm (30%,  $[\text{Re}(\text{NPh})\text{Cl}_3(\text{PPh}_3)_2]$ ). The filtrate was then evaporated to dryness and the  $^{31}\text{P}$  NMR spectrum of the residual recorded in  $\text{CD}_2\text{Cl}_2$ : 27.89 (10%,  $\text{Ph}_3\text{PO}$ ), 24.51 (4%),  $-4.97$  (15%,  $\text{PPh}_3$ ),  $-19.22$  (65%,  $[\text{Re}(\text{NPh})\text{Cl}_3(\text{PPh}_3)_2]$ ),  $-19.62$  ppm (10%).

**Refluxing of  $[\text{Re}(\text{NPh})\text{Cl}_3(\text{PPh}_3)_2]$  in Acetonitrile in the Presence of  $\text{Et}_3\text{NHCl}$ .** A suspension of  $[\text{Re}(\text{NPh})\text{Cl}_3(\text{PPh}_3)_2]$  (0.091 g, 0.100 mmol) and  $\text{Et}_3\text{NHCl}$  (0.041 g, 0.300 mmol) in acetonitrile (10 mL) was refluxed for 1 h. The green solid was filtered off and identified as pure  $[\text{Re}(\text{NPh})\text{Cl}_3(\text{PPh}_3)_2]$  by  $^{31}\text{P}$  NMR, and the  $^{31}\text{P}$  NMR spectrum of the filtrate was recorded in  $\text{CH}_3\text{CN}/\text{CD}_3\text{CN}$  (2:1, v:v):  $-4.55$  (43%,  $\text{PPh}_3$ ),  $-15.03$  (25%),  $-17.91$  (32%,  $[\text{Re}(\text{NPh})\text{Cl}_3(\text{PPh}_3)_2]$ ) ppm. The filtrate was then evaporated to dryness and the  $^{31}\text{P}$  NMR spectrum of the residual recorded in  $\text{CD}_2\text{Cl}_2$ : 27.89 (3%,  $\text{Ph}_3\text{PO}$ ), 24.51 (3%),  $-4.97$  (16%,  $\text{PPh}_3$ ),  $-10.13$  (1%,  $[\text{ReOCl}_3(\text{PPh}_3)_2]$ ),  $-19.22$  (68%,  $[\text{Re}(\text{NPh})\text{Cl}_3(\text{PPh}_3)_2]$ ),  $-19.62$  (3%),  $-24.71$  (7%) ppm.

**Refluxing of  $[\text{Re}(\text{NPh})\text{Cl}_3(\text{PPh}_3)_2]$  in Acetonitrile in the Presence of Triflic Acid.** A mixture of 0.091 g (0.100 mmol) of  $[\text{Re}(\text{NPh})\text{Cl}_3(\text{PPh}_3)_2]$  and 0.027 mL (0.300 mmol) of triflic acid was refluxed for 1 h in 10 mL of acetonitrile. The  $^{31}\text{P}$  NMR spectrum of the so-obtained green solution exhibited a single signal at  $-9.73$  ppm in  $\text{CH}_3\text{CN}/\text{CD}_3\text{CN}$  (2:1, v:v). The mother liquor was then evaporated to dryness, and the  $^{31}\text{P}$  NMR spectrum of the crude was recorded in  $\text{CD}_2\text{Cl}_2$ : 5.60 (16%),  $-4.97$  (2%,  $\text{PPh}_3$ ),  $-7.01$  (4%),  $-11.26$  ppm (78%). Crystals could be grown from the mother liquor at room temperature or at  $-30$  °C, possibly by slow diffusion of diethyl ether. Cell parameters, monoclinic  $P$ :  $a = 10.940$  Å;  $b = 27.376$  Å;  $c = 16.944$  Å;  $\beta = 103.8^\circ$ ;  $V = 4927$  Å<sup>3</sup>.

**Instrumentation and Techniques of Measurement.** IR spectra were recorded from KBr pellets on a Bio-Rad Win-IR FTS 165 FT-IR spectrophotometer, and UV-visible spectra were recorded on a Shimadzu UV-2101 spectrophotometer. The  $^1\text{H}$  (300 MHz) and  $^{31}\text{P}$  (121.5 MHz) NMR spectra were obtained at room temperature in 5 mm o.d. tubes on a Bruker AC 300 spectrometer

- (10) Proust, A.; Taunier, S.; Artero, V.; Robert, F.; Thouvenot, R.; Gouzerh, P. *Chem. Commun.* **1996**, 2195–2196.  
 (11) (a) Bushey, P. A. Thesis, Georgetown University, 1974. (b) Abrams, M. J.; Costello, C. E.; Shaikh, S. N.; Zubieta, J. *Inorg. Chim. Acta* **1991**, 180, 9–11. (c) Kwen, H.; Tomlinson, S.; Maatta, E. A.; Dablemont, C.; Thouvenot, R.; Proust, A.; Gouzerh, P. *Chem. Commun.* **2002**, 2970–2971.  
 (12) Radkov, E.; Beer, R. H. *Polyhedron* **1995**, 14, 2139–2143.  
 (13) Chatt, J.; Rowe, G. A. *J. Chem. Soc.* **1962**, 4019–4033.  
 (14) (a) Chatt, J.; Dilworth, J. R. *J. Chem. Soc., Chem. Commun.* **1972**, 549. (b) Goeden, G. V.; Haymore, B. L. *Inorg. Chem.* **1983**, 22, 157–167.

equipped with a QNP probehead. The chemical shifts are given according to the IUPAC convention with respect to  $\text{SiMe}_4$  for  $^1\text{H}$  NMR and to 85%  $\text{H}_3\text{PO}_4$  for  $^{31}\text{P}$  NMR. For  $^{31}\text{P}$  NMR, chemical shifts were determined by the substitution method. The  $^{14}\text{N}$  (36.13 MHz) NMR spectra were recorded at 300 K in  $\text{DMF}/\text{acetone}-d_6$  (7:1, v:v) solutions in 10 mm o.d. tubes on a Bruker AM 500 spectrometer, and the chemical shifts were given with respect to neat nitromethane. Electrochemical data were obtained in acetonitrile, with sample concentration of  $10^{-3}$  M and 0.1 M  $[\text{Bu}_4\text{N}]\text{-BF}_4$  as the supporting electrolyte. Cyclic voltammetry at a carbon electrode was carried out with a PAR model 273 instrument. A standard three-electrode cell was used, which consisted of the working electrode, an auxiliary platinum electrode, and an aqueous saturated calomel electrode (SCE) equipped with a double junction. All potentials are relative to SCE. The mass spectra were recorded using an ion trap mass spectrometer (Bruker Esquire 3000) equipped with an off-axis ESI source (Agilent). Negative mode was used for all experiments (capillary voltage 3500 V). Sample solutions ( $10 \text{ pmol}\cdot\mu\text{L}^{-1}$  in acetonitrile) were infused using a syringe pump into the ESI source at a flow rate of  $120 \mu\text{L}\cdot\text{h}^{-1}$ . The declustering was adjusted using the capillary exit-skimmer potential difference ( $\Delta\text{CE}_{\text{sk}}$ ). Typically a low declustering potential ( $\Delta\text{CE}_{\text{sk}} = 40 \text{ V}$ ) was used to keep the POM intact whereas higher values ( $\Delta\text{CE}_{\text{sk}} = 80 \text{ V}$ ) were used to obtain in-source decomposition. For full scan analysis the standard scan rate was used ( $13\,000 \text{ m/z}\cdot\text{s}^{-1}$ ) with an ion charge control (ICC) target set to 20 000. Under these conditions a peak width of almost 0.5 Da is obtained. A lower scan rate was used (enhanced mode,  $2000 \text{ m/z}\cdot\text{s}^{-1}$ ) together with a low ICC target (3000) to resolve multiply charged isotopic clusters. The X-ray diffraction powder patterns were recorded using a  $\text{Cu K}\alpha$  ( $\lambda = 1.5406 \text{ \AA}$ ) source. Scans were collected between  $2\theta = 2^\circ$  and  $2\theta = 80^\circ$  and counts measured for 20 s at each increment. Single-crystal cell data were recorded at room temperature on a CAD4 Enraf-Nonius diffractometer or a Nonius KAPPA CCD diffractometer with graphite-monochromated  $\text{Mo K}\alpha$  radiation ( $\lambda = 0.71069 \text{ \AA}$ ). The crystal was coated with paratone oil and glue and in some cases put in a Lindeman tube. Lattice parameters and the orientation matrix were obtained from at least-squares fit of 25 automatically centered reflections in the range  $12\text{--}12.2^\circ$ .

## Results and Discussion

### Synthesis and Stability of $[\text{Bu}_4\text{N}][\text{PW}_{11}\text{O}_{39}\{\text{Re}^{\text{V}}\text{NPh}\}]$

(1). A general procedure for the synthesis of monosubstituted Keggin tungstophosphates,  $[\text{PW}_{11}\text{O}_{39}\{\text{MO}\}]^{n-}$ , is based on the reaction of the monovacant species  $[\text{PW}_{11}\text{O}_{39}]^{7-}$  with a mononuclear oxo-halogeno-metal complex,  $[\text{MOX}_x]^{z-}$ . In this way, Pope et al.<sup>15</sup> have obtained  $[\text{Bu}_4\text{N}][\text{PW}_{11}\text{O}_{39}\{\text{Re}^{\text{V}}\text{O}\}]$  (**2**) from  $[\text{Bu}_4\text{N}]_4[\text{H}_3\text{PW}_{11}\text{O}_{39}]$ <sup>12</sup> and  $[\text{Bu}_4\text{N}][\text{Re}^{\text{V}}\text{OBr}_4]$ .<sup>16</sup> We have found that the reaction also works with the molecular  $[\text{ReOCl}_3(\text{PPh}_3)_2]$  complex, which has the advantage of being prepared in a nearly quantitative yield.<sup>13</sup> The purity of **2** was checked by  $^{31}\text{P}$  NMR, recorded in  $\text{CD}_3\text{-CN}$  (see Supporting Information). Using an analogous procedure with  $[\text{Re}(\text{NPh})\text{Cl}_3(\text{PPh}_3)_2]$ , which was refluxed for 1 h with  $[\text{Bu}_4\text{N}]_4[\text{H}_3\text{PW}_{11}\text{O}_{39}]$  in distilled acetonitrile, under argon, and in the presence of triethylamine, we have now obtained the first Keggin-type organoimido derivative  $[\text{Bu}_4\text{N}][\text{PW}_{11}\text{O}_{39}\{\text{Re}^{\text{V}}\text{NPh}\}]$  (**1**) (Figure 1). However, **1** proved to

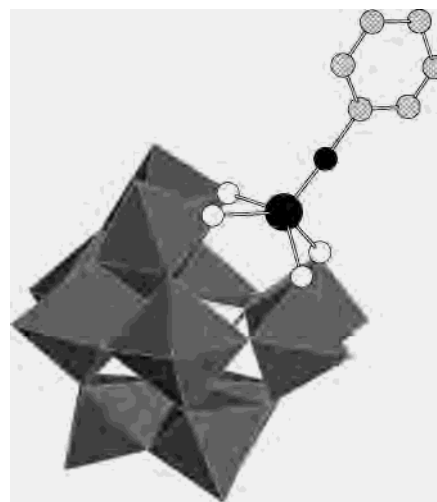


**Figure 1.** Probable structure of  $[\text{PW}_{11}\text{O}_{39}\{\text{ReNPh}\}]^{4-}$  in a polyhedral representation.

be systematically contaminated with  $[\text{Bu}_4\text{N}]_4[\text{PW}_{11}\text{O}_{39}\{\text{Re}^{\text{V}}\text{O}\}]$  (**2**) (see below). Besides the signal attributed to **1** and **2**, the  $^{31}\text{P}$  NMR spectrum of the deep purple reactant solution further displays a signal attributed to  $\text{PPh}_3$ . No evidence has been found for the formation of  $\text{Ph}_3\text{PO}$ . Crystals were grown by slow diffusion of diethyl ether into the mother liquor. Any attempted recrystallization has up to now failed to separate **1** from **2**. Three different hypothesis have been considered to account for the presence of **2** in the product of the reaction of  $[\text{Re}(\text{NPh})\text{Cl}_3(\text{PPh}_3)_2]$  with  $[\text{Bu}_4\text{N}]_4[\text{H}_3\text{PW}_{11}\text{O}_{39}]$ : (i) inadvertent contamination of the starting compound  $[\text{Re}(\text{NPh})\text{Cl}_3(\text{PPh}_3)_2]$  with  $[\text{ReOCl}_3(\text{PPh}_3)_2]$ ; (ii) hydrolysis of  $[\text{Re}(\text{NPh})\text{Cl}_3(\text{PPh}_3)_2]$  in the course of the reaction; (iii) hydrolysis of **1** once formed.

The rhenium precursor  $[\text{Re}(\text{NPh})\text{Cl}_3(\text{PPh}_3)_2]$  was synthesized according to the published procedure<sup>14</sup> by reaction of  $\text{Ph}_3\text{PNPh}$  on  $[\text{ReOCl}_3(\text{PPh}_3)_2]$  but using toluene as the solvent instead of benzene. This resulted in a decrease of the solubility of  $[\text{Re}(\text{NPh})\text{Cl}_3(\text{PPh}_3)_2]$ , which precipitated during the reaction. Further crops of product were later collected to attain a whole yield of 82%. While  $[\text{ReOCl}_3(\text{PPh}_3)_2]$  is quite insoluble in acetonitrile and only sparingly soluble in chlorinated solvents, the imido derivative  $[\text{Re}(\text{NPh})\text{Cl}_3(\text{PPh}_3)_2]$  is more soluble in organic solvents and is characterized by a single  $^{31}\text{P}$  NMR signal at  $-19.22 \text{ ppm}$  in  $\text{CH}_2\text{Cl}_2/\text{CD}_2\text{Cl}_2$  (2:1, v:v) and at  $-17.91 \text{ ppm}$  in  $\text{CH}_3\text{CN}/\text{CD}_3\text{CN}$  (2:1, v:v). This is at variance with  $[\text{ReOCl}_3(\text{PPh}_3)_2]$ , whose  $^{31}\text{P}$  NMR spectrum displays two peaks at  $-10.13 \text{ ppm}$  (relative intensity 40%) and  $-18.44 \text{ ppm}$  (60%) in  $\text{CH}_2\text{Cl}_2/\text{CD}_2\text{Cl}_2$  (2:1, v:v), reflecting the existence of two isomers in solution.<sup>13</sup> Neither the  $^{31}\text{P}$  NMR signature of  $[\text{ReOCl}_3(\text{PPh}_3)_2]$  nor the characteristic  $\nu(\text{ReO})$  IR band at  $969 \text{ cm}^{-1}$  could be observed in the spectra of the imido samples, which indicates that the later was isolated free of the parent oxo complex.

The stability of  $[\text{Re}(\text{NPh})\text{Cl}_3(\text{PPh}_3)_2]$  in refluxing acetonitrile has been assessed, first in the absence of any other reagent and then in the presence of triethylammonium chloride, since triethylammonium is formed by reaction of triethylamine with  $[\text{Bu}_4\text{N}]_4[\text{H}_3\text{PW}_{11}\text{O}_{39}]$  in the synthesis

(15) Ortéga, F.; Pope, M. T. *Inorg. Chem.* **1984**, *23*, 3292–3297.

(16) Cotton, F. A.; Lippard, S. J. *Inorg. Chem.* **1966**, *1*, 9–16.

procedure. In any control experiment, a suspension was obtained. The solid was identified as pure  $[\text{Re}(\text{NPh})\text{Cl}_3(\text{PPh}_3)_2]$  by IR and  $^{31}\text{P}$  NMR spectroscopy. In addition to the signal of  $[\text{Re}(\text{NPh})\text{Cl}_3(\text{PPh}_3)_2]$ , the  $^{31}\text{P}$  NMR spectrum of the filtrate displayed the signal of free  $\text{PPh}_3$  at  $-4.55$  ppm and another unidentified signal at  $15.03$  ppm, which provides evidence for some transformation of  $[\text{Re}(\text{NPh})\text{Cl}_3(\text{PPh}_3)_2]$ . The filtrate was then evaporated to dryness, and the residue was characterized by IR and  $^{31}\text{P}$  NMR spectroscopy, in  $\text{CD}_2\text{-Cl}_2$ . Neither the IR spectra of the crude samples obtained by evaporation of acetonitrile nor those of the initial precipitates exhibited the  $\nu(\text{ReO})$  characteristic band. The oxo complex  $[\text{ReOCl}_3(\text{PPh}_3)_2]$  was only detected in the experiment carried out in the presence of triethylammonium chloride but in a small amount (less than 1%), which could clearly not account for the formation of **2**, sometimes obtained in more than 20%.

Refluxing  $[\text{Re}(\text{NPh})\text{Cl}_3(\text{PPh}_3)_2]$  in the presence of triflic acid resulted in a green solution and according to  $^{31}\text{P}$  NMR in the formation of a single phosphorus-containing product, but which does correspond to neither  $[\text{Re}(\text{NPh})\text{Cl}_3(\text{PPh}_3)_2]$  nor  $[\text{ReOCl}_3(\text{PPh}_3)_2]$ . No  $\nu(\text{ReO})$  band could be recognized by IR. Crystals were obtained by slow evaporation of the mother liquor, but their decay, probably due to the loss of solvent molecules, prevented a full X-ray diffraction analysis.

The last point to examine was the intrinsic stability of **1** toward hydrolysis. Although acetonitrile was distilled over calcium hydride prior to use, it should contain some residual water. In a control experiment, distilled water, up to 0.05 mL (large excess), was intentionally added to the reaction mixture. This did not appear to modify drastically the relative proportions of **1** and **2** in the product, as shown by  $^1\text{H}$  NMR. However, two observations led us to conclude that **1** is indeed moisture sensitive in the solid state, even if it does not transform into  $[\text{Bu}_4\text{N}]_4[\text{PW}_{11}\text{O}_{39}\{\text{ReO}\}]$  (**2**) but to a yet unidentified compound. First, after 5 months, solid samples of  $[\text{Bu}_4\text{N}]_4[\text{PW}_{11}\text{O}_{39}\{\text{Re}^{\text{V}}\text{NPh}\}]$  (**1**), stored without any special care, showed a modified  $^{31}\text{P}$  NMR spectrum in  $\text{CD}_3\text{-CN}$  with a broad signal at  $-14$  ppm (relative intensity 70%,  $\Delta\nu_{1/2} = 40$  Hz) and the sharp signal at  $-14.59$  ppm (28%,  $\Delta\nu_{1/2} = 1$  Hz). This evolution could also be followed by  $^1\text{H}$  NMR by the broadening of the signals due to the aromatic protons of the imido function. A similar behavior was observed by washing collected crystals of  $[\text{Bu}_4\text{N}]_4[\text{PW}_{11}\text{O}_{39}\{\text{ReNPh}\}]$  (**1**) with water, for the purpose of eliminating triethylammonium chloride. Samples of  $[\text{Bu}_4\text{N}]_4[\text{PW}_{11}\text{O}_{39}\{\text{ReNPh}\}]$  (**1**) should then be stored under argon. The signal at  $-14$  ppm has not been assigned. It corresponds to neither  $[\text{Bu}_4\text{N}]_4[\text{PW}_{11}\text{O}_{39}\{\text{Re}^{\text{V}}\text{O}\}]$  (**2**) nor the oxidized  $[\text{Bu}_4\text{N}]_4[\text{PW}_{11}\text{O}_{39}\{\text{Re}^{\text{VI}}\text{O}\}]$ , which resonates at  $-18$  ppm and which also gives a broad peak ( $\Delta\nu_{1/2} = 50$  Hz) because of its paramagnetism.

**Protonation States of  $[\text{PW}_{11}\text{O}_{39}]^{7-}$ .** Even if the presence of the protons in the starting  $[\text{Bu}_4\text{N}]_4[\text{H}_3\text{PW}_{11}\text{O}_{39}]$  could not be definitively related to the formation of contaminating  $[\text{Bu}_4\text{N}]_4[\text{PW}_{11}\text{O}_{39}\{\text{ReO}\}]$  (**2**), we thought of getting rid of them by simple deprotonation with a base. We have thus followed by  $^{31}\text{P}$  NMR the addition of  $[\text{Bu}_4\text{N}]\text{OH}$  to an

acetonitrile solution of  $[\text{Bu}_4\text{N}]_4[\text{H}_3\text{PW}_{11}\text{O}_{39}]$ . A similar study was performed on the molybdenum analogue  $[\text{Bu}_4\text{N}]_4[\text{H}_3\text{-PMo}_{11}\text{O}_{39}]$  by Hill et al.<sup>17</sup> The spectra were recorded for solutions initially  $10^{-2}$  M in polyanion in a  $\text{CH}_3\text{CN}/\text{CD}_3\text{CN}$  (2:1, v:v) mixture. Under these conditions,  $[\text{Bu}_4\text{N}]_4[\text{H}_3\text{-PW}_{11}\text{O}_{39}]$  was found to resonate at  $-12.04$  ppm. Addition of 1 equiv of  $[\text{Bu}_4\text{N}]\text{OH}$ , from a 0.1 M solution in methanol, cleanly led to a single signal at  $-11.52$  ppm, which we have attributed to  $[\text{H}_2\text{PW}_{11}\text{O}_{39}]^{5-}$ . Further deprotonation was not easily achieved since addition of increasing equivalents of base from 2 to 5 resulted in each case in a mixture of compounds, namely  $[\text{H}_2\text{PW}_{11}\text{O}_{39}]^{5-}$  and two other compounds, which resonate at  $-10.60$  and  $-9.14$  ppm. Deprotonation of  $[\text{H}_3\text{PW}_{11}\text{O}_{39}]^{4-}$  to  $[\text{H}_2\text{PW}_{11}\text{O}_{39}]^{5-}$  results in a shift of  $+0.52$  ppm. If the difference of  $+0.92$  ppm between  $-11.52$  and  $-10.60$  ppm could tentatively correspond to a further deprotonation, going on from  $[\text{H}_2\text{PW}_{11}\text{O}_{39}]^{5-}$  to  $[\text{HPW}_{11}\text{O}_{39}]^{6-}$ , the difference of  $+2.38$  ppm with the signal at  $-9.14$  ppm would rather indicate the formation of another species, possibly a multivacant polyanion.<sup>18</sup> Whatever the number of  $[\text{Bu}_4\text{N}]\text{OH}$  equivalents added to the solution of polyanion, from 3 to 5, the ratio  $[\text{H}_2\text{PW}_{11}\text{O}_{39}]^{5-}/[\text{HPW}_{11}\text{O}_{39}]^{6-}$  remained almost unchanged, the sign of an equilibrium. This probably reflects the similar basicities of  $\text{OH}^-$  and  $[\text{HPW}_{11}\text{O}_{39}]^{6-}$ . On the other hand, the degradation of the  $\text{PW}_{11}$  skeleton, if evidenced by the signal at  $-9.14$  ppm, could be tentatively related to the absence of a suitable cation other than the protons to stabilize the vacancy. This should be avoided in the presence of an alkali metal cation, for example. This led us to use LiOMe as a base to assess both the effect of a lithium cation and the effect of a base stronger than  $[\text{Bu}_4\text{N}]\text{OH}$ . Comparing the spectra obtained with increasing equivalents of LiOMe to the previous ones resulted in the following observations: (i) The chemical shifts are globally positively shifted. (ii) Whatever the number of LiOMe equivalents added, the spectra display several signals. (iii) Some of these signals are broad. Points i and iii probably reveal some interaction between vacant polyanions and lithium cations. However a full assignment of the spectra would have required more detailed complementary studies, varying independently the strength of the base added and the nature of the alkali metal cation. These were not undertaken, all the more that no indication in favor of the formation of a fully deprotonated and quantitatively generated species could be inferred from the experimental data.

As an alternative to the use of  $[\text{Bu}_4\text{N}]_4[\text{H}_3\text{PW}_{11}\text{O}_{39}]$ , we could have started with the parent  $[\text{Bu}_4\text{N}]_3[\text{PW}_{12}\text{O}_{40}]$  and generated in situ vacant polyanions by addition of tetrabutylammonium hydroxide. This method was initially described by Pope et al. for the synthesis of rhenium derivatives<sup>19</sup> and was latter successfully applied in our group to the synthesis

(17) Combs-Walker, L. A.; Hill, C. L. *Inorg. Chem.* **1991**, *30*, 4016–4026.

(18) (a) Massart, R.; Contant, R.; Fruchart, J.-M.; Ciabrini, J.-P.; Fournier, M. *Inorg. Chem.* **1977**, *16*, 2916–2921. (b) Mazeaud, A.; Ammari, N.; Robert, F.; Thouvenot, R. *Angew. Chem., Int. Ed. Engl.* **1996**, *35*, 1961–1964; *Angew. Chem.* **1996**, *108*, 2089–2092. (c) Mayer, C. R.; Thouvenot, R. *J. Chem. Soc., Dalton Trans.* **1998**, 7–14.

(19) Meiklejohn, P. T.; Pope, M. T.; Prados, R. A. *J. Am. Chem. Soc.* **1974**, *21*, 6779–6781.

of the nitrosyl derivatives  $[\text{Bu}_4\text{N}]_4[\text{PW}_{11}\text{O}_{39}\{\text{MoNO}\}]$  at room temperature<sup>20</sup> and very recently to the preparation of the organodiazenido Keggin derivatives  $[\text{Bu}_4\text{N}]_4[\text{PW}_{11}\text{O}_{39}\{\text{MoN}_2\text{Ar}\}]$ .<sup>21</sup> However, addition of 5 equiv of  $[\text{Bu}_4\text{N}]\text{OH}$  to a solution of  $[\text{Bu}_4\text{N}]_3[\text{PW}_{12}\text{O}_{40}]$  cleanly produces  $[\text{H}_2\text{PW}_{11}\text{O}_{39}]^{5-}$  as the sole product, which brought us back to the system we have previously described. Starting from  $[\text{Bu}_4\text{N}]_3[\text{PW}_{12}\text{O}_{40}]$  does not apparently provide any alternative.

Following the conclusion of the very first NMR experiment, we could prepare  $[\text{Bu}_4\text{N}]_5[\text{H}_2\text{PW}_{11}\text{O}_{39}]$ , quantitatively and at a millimolar scale, by reaction of 1 equiv of  $[\text{Bu}_4\text{N}]\text{OH}$  with 1 equiv of  $[\text{Bu}_4\text{N}]_4[\text{H}_3\text{PW}_{11}\text{O}_{39}]$  in acetonitrile solution and evaporation of the solvent to dryness. It is then soluble in dichloromethane and thus provides a convenient precursor to work in solvents less polar than those usually used in polyoxometalate chemistry. Similarly, addition of 3 equiv of triethylamine to a solution of  $[\text{Bu}_4\text{N}]_4[\text{H}_3\text{PW}_{11}\text{O}_{39}]$  in acetonitrile, as described herein for the synthesis of  $[\text{Bu}_4\text{N}]_4[\text{PW}_{11}\text{O}_{39}\{\text{ReNPh}\}]$  (**1**), was shown by <sup>31</sup>P NMR to produce  $[\text{H}_2\text{PW}_{11}\text{O}_{39}]^{5-}$ , as characterized by a single signal at  $-11.52$  ppm.

**Characterization.** Since  $[\text{Bu}_4\text{N}]_4[\text{PW}_{11}\text{O}_{39}\{\text{Re}^{\text{V}}\text{NPh}\}]$  (**1**) and  $[\text{Bu}_4\text{N}]_4[\text{PW}_{11}\text{O}_{39}\{\text{Re}^{\text{V}}\text{O}\}]$  (**2**) are closely related, the features of **1** have been discussed by comparison with those of **2**. Furthermore, as samples of **1** were found to be systematically contaminated by **2**, features of **2**, once recognized, have also been used as internal standard.

**IR Spectroscopy.** The IR spectra of **1** and **2** are quite similar and display the characteristic features of a Keggin-type structure: five strong vibration bands are indeed observed, at  $1076$  and  $963$   $\text{cm}^{-1}$  and in the range  $885$ – $775$   $\text{cm}^{-1}$ , which are assigned to  $\nu(\text{PO})$ ,  $\nu(\text{M}=\text{O})$ , and  $\nu(\text{M}-\text{O}-\text{M})$  stretching modes, respectively.<sup>22a,b</sup> Compared to  $[\text{Bu}_4\text{N}]_3[\text{PW}_{12}\text{O}_{40}]$ , the IR spectrum of **1** displays a shoulder on the  $\nu(\text{PO})$  band at  $1045$   $\text{cm}^{-1}$ , as a consequence of the introduction of the rhenium(V) cation (ionic radius  $5.8 \times 10^{-1}$  Å) slightly smaller than a tungsten(VI) (ionic radius  $6.0 \times 10^{-1}$  Å) and thus not able to refill completely the vacancy of  $[\text{PW}_{11}\text{O}_{39}]^{7-}$ .<sup>22c</sup> In the spectrum of **2**, this shoulder appears at  $1058$   $\text{cm}^{-1}$ .

**UV–Visible Spectroscopy.** The electronic spectrum of **1** in acetonitrile solution displays two bands at  $532$  nm ( $\log \epsilon \sim 3.5$ ) and  $728$  nm ( $\log \epsilon \sim 3.1$ ), showing a bathochromic shift with respect to the corresponding bands of **2**, which were found at  $510$  nm ( $\log \epsilon \sim 3.5$ ) and  $688$  nm ( $\log \epsilon \sim 3.2$ ), in agreement with the literature, and which have been attributed by Pope et al. to rhenium(V) to tungsten(VI) intervalence transitions.<sup>19</sup> The observed bathochromic shift is consistent with the trend in  $\pi$ -donor ability of the ligands.<sup>23</sup>

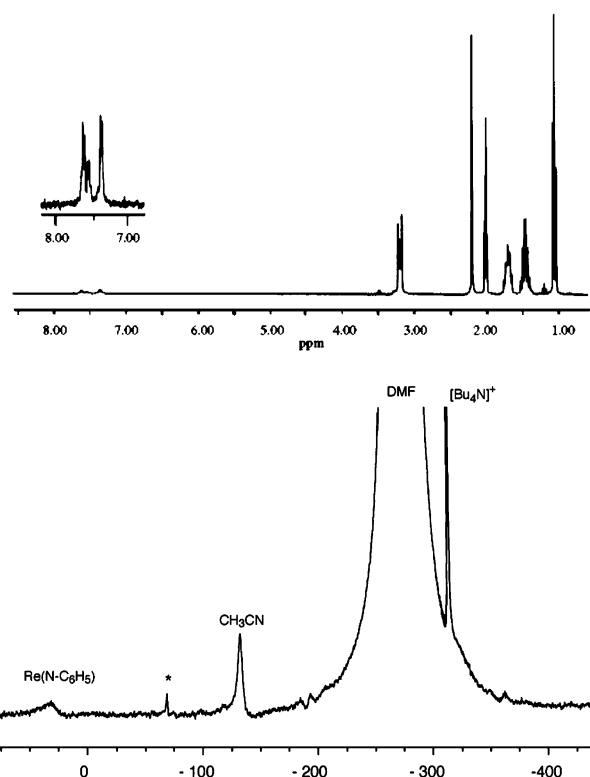


**Figure 2.** <sup>1</sup>H (top) and <sup>14</sup>N (bottom) NMR spectra of  $[\text{Bu}_4\text{N}]_4[\text{PW}_{11}\text{O}_{39}\{\text{Re}^{\text{V}}\text{NPh}\}]$  (**1**) (in  $\text{CD}_3\text{CN}$  and  $\text{DMF}/\text{acetone-}d_6$ , respectively). The resonance indicated by an asterisk corresponds to a spurious signal, likely due to an electronic artifact.

The d–d transition further observed for **2** at  $387$  nm ( $\log \epsilon \sim 3.2$ ) is hidden by LMCT processes in the case of **1**.

**Multinuclear NMR Spectroscopy.** The formation of a phenylimido derivative is demonstrated without any ambiguity by <sup>1</sup>H and <sup>14</sup>N NMR (see Figure 2). The <sup>1</sup>H NMR spectrum, recorded in  $\text{CD}_3\text{CN}$ , displays three signals at  $7.59$ ,  $7.51$ , and  $7.34$  ppm for the phenyl group. On the other hand, the <sup>14</sup>N NMR spectrum of **1** further confirms the presence of the imido ligand displaying a signal at  $30$  ppm in a  $\text{DMF}/\text{acetone-}d_6$  (7:1, v:v) mixture. This chemical shift is in agreement with those previously reported for the functionalized Lindqvist-type POMs  $[\text{Bu}_4\text{N}]_2[\text{Mo}_6\text{O}_{19-x}(\text{NPh})_x]$ .<sup>4,8</sup> However, in both the <sup>1</sup>H and <sup>14</sup>N spectra the ratio between their relative intensities and those of the tetrabutylammonium cations indicates the presence of an excess of  $\text{Bu}_4\text{N}^+$  cations. That **2** is indeed the impurity present in samples of **1** was inferred from <sup>31</sup>P NMR: samples of **1** in acetonitrile are characterized by a single signal at  $-14.59$  ppm, which thus appears to coincide with that of **2**. The ratio of **1** to **2** was usually deduced from the <sup>1</sup>H NMR by comparison of the relative intensities of the signals arising from the aromatic protons and the tetrabutylammonium cations. The contamination rate slightly varies from one sample to one another and is about 20–25%.

**Cyclic Voltammetry.** Characterization of **1** by cyclic voltammetry, in acetonitrile and at a carbon electrode, confirms that all the samples are contaminated by **2**. The signature of  $[\text{Bu}_4\text{N}]_4[\text{PW}_{11}\text{O}_{39}\{\text{ReNPh}\}]$  (**1**) could then be obtained only after subtraction of that of **2**. Three quasi-

(20) Proust, A.; Fournier, M.; Thouvenot, R.; Gouzerh, P. *Inorg. Chim. Acta* **1994**, *215*, 61–66.

(21) Bustos, C.; et al. Manuscript in preparation

(22) (a) Rocchiccioli-Deltcheff, C.; Thouvenot, R.; Franck, R. *Spectrochim. Acta* **1976**, *32 A*, 587–597. (b) Rocchiccioli-Deltcheff, C.; Franck, R.; Fournier, R.; Thouvenot, R. *Inorg. Chem.* **1983**, *22*, 207–216. (c) Rocchiccioli-Deltcheff, C.; Thouvenot, R. *J. Chem. Res., Synop.* **1977**, *46*; *J. Chem. Res., Miniprint* **1977**, 549.

(23) Nugent, W.; Mayer, J. E. *Metal–Ligand Multiple Bonds*; Wiley: New York, 1988; Chapter 4, p 112.

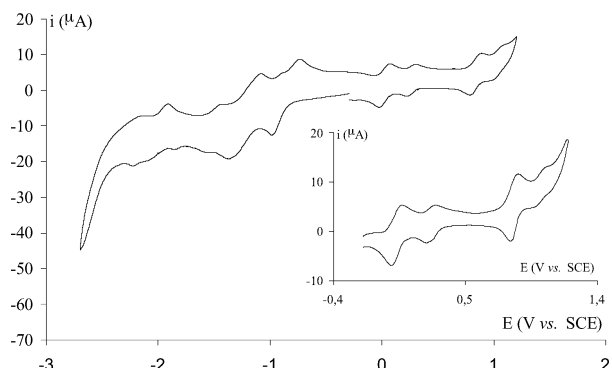


**Figure 3.** Complete cyclic voltammogram (top) and oxidation waves (bottom) of  $[\text{Bu}_4\text{N}]_4[\text{PW}_{11}\text{O}_{39}\{\text{Re}^{\text{V}}\text{NPh}\}]$  (**1**) contaminated by  $[\text{Bu}_4\text{N}]_4[\text{PW}_{11}\text{O}_{39}\{\text{Re}^{\text{V}}\text{O}\}]$  (**2**) (1 mM in  $\text{CH}_3\text{CN}$ , 0.1 M  $[\text{Bu}_4\text{N}]\text{BF}_4$ ,  $E$  in V vs SCE at a carbon electrode,  $100 \text{ mV}\cdot\text{s}^{-1}$ ).

**Table 1.** Electrochemical Data in V vs SCE in  $\text{CH}_3\text{CN}$  in Samples of **1** Contaminated by **2**

wave	$[\text{PW}_{11}\text{O}_{39}\{\text{Re}^{\text{V}}\text{NPh}\}]^{4-}$ (anion of <b>1</b> )		$[\text{PW}_{11}\text{O}_{39}\{\text{Re}^{\text{V}}\text{O}\}]^{4-}$ (anion of <b>2</b> )	
	$\text{Re}^{7+}/\text{Re}^{6+}$	$\text{Re}^{6+}/\text{Re}^{5+}$	$\text{Re}^{7+}/\text{Re}^{6+}$	$\text{Re}^{6+}/\text{Re}^{5+}$
$E_{\text{pa}}$	0.86	0.06	1.04	0.29
$E_{\text{pc}}$	0.81	-0.01	0.97	0.24
$1/2(E_{\text{pa}} + E_{\text{pc}})$	0.84	0.03	1.01	0.27
$E_{\text{pa}} - E_{\text{pc}}$	0.05	0.07	0.07	0.05

reversible waves at 1.12, 0.35, and  $-0.80$  V and two irreversible ones at  $-1.37$  and  $-1.91$  V (vs SCE) are observed in the voltammogram of pure  $[\text{Bu}_4\text{N}]_4[\text{PW}_{11}\text{O}_{39}\{\text{Re}^{\text{V}}\text{O}\}]$  (**2**), recorded in acetonitrile, in agreement with the characterization reported in the literature.<sup>15</sup> The first four waves are one-electron processes and were assigned to the  $\text{Re}^{7+}/\text{Re}^{6+}$ ,  $\text{Re}^{6+}/\text{Re}^{5+}$ ,  $\text{Re}^{5+}/\text{Re}^{4+}$ , and  $\text{Re}^{4+}/\text{Re}^{3+}$  couples, respectively, while the latter is a multielectron process attributed to the reduction of the polyoxotungstate framework. Compound **1** is thus characterized by two quasi-reversible oxidation processes at 0.84 and 0.03 V (vs SCE), ascribed to the oxidation of  $\text{Re}^{6+}$  to  $\text{Re}^{7+}$  and of  $\text{Re}^{6+}$  to  $\text{Re}^{5+}$ , respectively (see Figure 3 and Table 1). The cathodic shift when compared to the similar processes involved in **2** follows the trend in  $\pi$ -donor ability of the ligands, i.e.  $\text{O}^{2-} < \text{RN}^{2-}$ .<sup>23</sup> Separation of **1** from **2** contributions is less easy for the rest of the voltammogram since the reduction waves are rather ill-defined. We can indeed expect the effect of the variation in the  $\pi$ -donor character of the ligands to decrease with the oxidation states of the rhenium.

**ESI-Mass Spectrometry.** The mass spectrum of **2** shows three isotopic clusters centered at  $m/z$  960 (100%), 1561 (5%), and 1682 (2%). On one hand, a better resolution can be obtained by decreasing the ion number in the ion trap and the scanning rate (from 13 000 to  $2000 \text{ m/z}\cdot\text{s}^{-1}$ ). The corresponding spectrum displays molecular peaks regularly spaced with  $\Delta(m/z) = 1/3$ , for  $m/z$  960, which implies a 3-charge. On the other hand, as already observed with the  $[\text{Bu}_4\text{N}]^+$  salt of  $[\alpha_2\text{-P}_2\text{W}_{17}\text{O}_{61}\{\text{Re}^{\text{V}}\text{O}\}]$ ,<sup>6-24</sup> the two signals at  $m/z$  1561 and 1682 are due to aggregates between the POM and the  $[\text{Bu}_4\text{N}]^+$  cation. However, the complete assignment

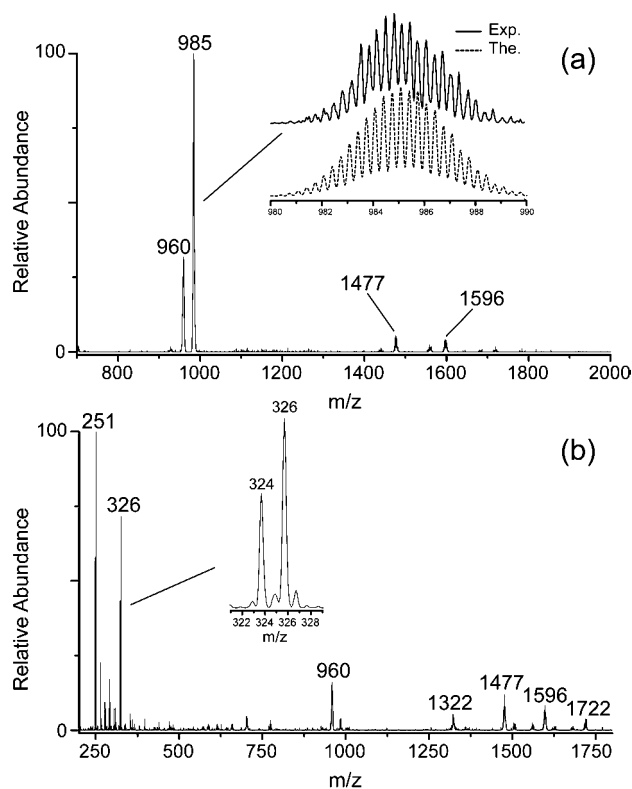


**Figure 4.** Negative mode electrospray mass spectrum of a  $10 \text{ pmol}\cdot\mu\text{L}^{-1}$   $\text{CH}_3\text{CN}$  solution of  $[\text{Bu}_4\text{N}]_4[\text{PW}_{11}\text{O}_{39}\{\text{Re}^{\text{V}}\text{NPh}\}]$  (**1**) recorded under (a) lower and (b) higher declustering conditions.

of the spectrum is still ambiguous. For example, the isotopic mass pattern at  $m/z$  960 can be attributed both to  $[\text{PW}_{11}\text{O}_{39}\{\text{Re}^{\text{V}}\text{O}\}]^{3-}$  anion or to  $[\text{HPW}_{11}\text{O}_{39}\{\text{Re}^{\text{V}}\text{O}\}]^{3-}$ . Indeed, the broadness of the signals and the complexity of the isotopic pattern does not allow the discrimination between a non- and a monoprotonated species. This led to some ambiguity for the attribution of the rhenium oxidation state (i.e.  $\text{Re}^{\text{V}}$  or  $\text{Re}^{\text{VI}}$ ). However, the isotopic mass pattern at  $m/z$  1682 can only be assigned to the  $[\text{Bu}_4\text{N}]_2[\text{PW}_{11}\text{O}_{39}\{\text{Re}^{\text{V}}\text{O}\}]^{2-}$  aggregate and the oxidation state should not vary from one  $[\text{PW}_{11}\text{O}_{39}\{\text{Re}^{\text{V}}\text{O}\}]^n$  cluster to one another. As a consequence, we have attributed the signals at  $m/z$  960, 1561, and 1682 to  $[\text{HPW}_{11}\text{O}_{39}\{\text{Re}^{\text{V}}\text{O}\}]^{3-}$ ,  $[\text{Bu}_4\text{N}][\text{HPW}_{11}\text{O}_{39}\{\text{Re}^{\text{V}}\text{O}\}]^{2-}$ , and  $[\text{Bu}_4\text{N}]_2[\text{PW}_{11}\text{O}_{39}\{\text{Re}^{\text{V}}\text{O}\}]^{2-}$ , respectively.

Mass spectra of samples of  $[\text{Bu}_4\text{N}]_4[\text{PW}_{11}\text{O}_{39}\{\text{Re}^{\text{V}}\text{NPh}\}]$  (**1**) confirm the functionalization but also reveal the presence of **2** as an impurity (see Figure 4). Indeed, under soft declustering conditions, spectra show two main signals at  $m/z$  985 (100%) and 960 (32%) attributed respectively to  $[\text{HPW}_{11}\text{O}_{39}\{\text{Re}^{\text{V}}\text{NPh}\}]^{3-}$  and  $[\text{HPW}_{11}\text{O}_{39}\{\text{Re}^{\text{V}}\text{O}\}]^{3-}$ . To a lesser extent, three signals are observed corresponding to  $[\text{H}_2\text{PW}_{11}\text{O}_{39}\{\text{Re}^{\text{V}}\text{NPh}\}]^{2-}$  ( $m/z$  1477, 5%),  $[\text{Bu}_4\text{N}][\text{HPW}_{11}\text{O}_{39}\{\text{Re}^{\text{V}}\text{O}\}]^{2-}$  ( $m/z$  1561, 2%), and  $[\text{Bu}_4\text{N}][\text{HPW}_{11}\text{O}_{39}\{\text{Re}^{\text{V}}\text{NPh}\}]^{2-}$  ( $m/z$  1596, 4%). Under these conditions, the structure of the POM and its functionalization are maintained in the gas phase. As previously, the charges state (3-) was confirmed by recording a mass spectrum using a slower scanning rate for the signal of **1** at  $m/z$  985. Using a relatively high declustering potential, in source decomposition is obtained. Low mass-to-charge ratio ions are displayed at  $m/z$

(24) Venturelli, A.; Nilges, M. J.; Smirnov, A.; Belford, R. L.; Francesconi, L. C. *J. Chem. Soc., Dalton Trans.* **1999**, 301–310.

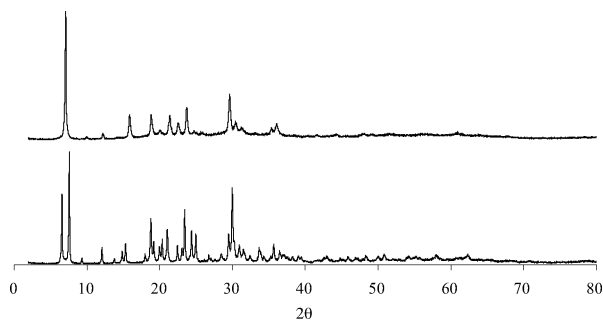


**Figure 5.** X-ray diffraction powder diagrams of  $[\text{Bu}_4\text{N}]_4[\text{PW}_{11}\text{O}_{39}\{\text{Re}^{\text{V}}\text{-NPh}\}]$  (**1**) (top) and  $[\text{Bu}_4\text{N}]_4[\text{PW}_{11}\text{O}_{39}\{\text{Re}^{\text{V}}\text{O}\}]$  (**2**) (bottom).

326 (72%) and  $m/z$  251 (100%), which are assigned to  $[\text{Re}^{\text{VI}}\text{O}_3(\text{NPh})]^-$  and  $[\text{Re}^{\text{VII}}\text{O}_4]^-$  (see Figure 3b) as demonstrated by the characteristic isotopic pattern of rhenium. The former confirms the presence of the metal–nitrogen multiple bond.

**Crystallographic Studies.** The X-ray diffraction powder diagram of **2** (Figure 5) can be indexed in a tetragonal  $I$  ( $a = 18.8 \text{ \AA}$ ;  $c = 14.7 \text{ \AA}$ ) cell. As the cell determined by single-crystal X-ray diffraction is cubic  $I$  ( $a = 17.76(1) \text{ \AA}$ ;  $V = 5599(7) \text{ \AA}^3$ ), the crystal crushing to powder seems to induce a phase transition. Surprisingly, the powder diagram recorded for **1** did not display any contribution of **2** and could be cleanly indexed in a cubic  $I$  mode ( $a = 17.6 \text{ \AA}$ ), which would be in favor of a syncrystallization of **1** and **2** rather than a cocrystallization. Syncrystallization is preceded for organoimido derivatives of the Lindqvist hexamolybdate.<sup>4a</sup> The X-ray diffraction powder diagrams have been indexed using the program Carine Crystallography, and calculated and experimental values are compared in the Supporting Information. However, an evolution of the starting sample was evidenced by the  $^{31}\text{P}$  NMR spectrum of the powder, recorded after X-ray irradiation, and which displayed a main and broad peak at  $-14.46 \text{ ppm}$  (87%,  $\Delta\nu_{1/2} = 15 \text{ Hz}$ ) together with the sharp peak attributed to **1**, as well as **2**, at  $-14.59 \text{ ppm}$  (13%,  $\Delta\nu_{1/2} = 1 \text{ Hz}$ ) and which was the only one detected before irradiation. According to  $^1\text{H}$  NMR, the starting sample of **1** was estimated to be contaminated with 25% **2**, which could tentatively account for the remaining signal at  $-14.59 \text{ ppm}$  in the  $^{31}\text{P}$  NMR spectrum, after irradiation. After irradiation, the NMR signals attributed to the aromatic protons were ill-resolved, while those of the tetrabutylammonium cations remained well-defined. On the other hand, the mass spectrum recorded with the powder after irradiation

was similar to that of the starting sample, with three patterns at  $m/z = 960$  (55%), 985 (100%), and 1596 (28%). No other pattern could be detected. These patterns have been previously attributed to  $[\text{HPW}_{11}\text{O}_{39}\{\text{Re}^{\text{VO}}\}]^{3-}$ ,  $[\text{HPW}_{11}\text{O}_{39}\{\text{Re}^{\text{V}}\text{NPh}\}]^{3-}$ , and  $[\text{Bu}_4\text{N}][\text{HPW}_{11}\text{O}_{39}\{\text{Re}^{\text{V}}\text{NPh}\}]^{3-}$ , respectively. However, to be in agreement with the change observed in  $^{31}\text{P}$  NMR and especially with the broadening of the signal, which suggests the presence of a paramagnetic species, the two latter, after X-ray irradiation, should rather correspond to the nonprotonated but oxidized anions  $[\text{PW}_{11}\text{O}_{39}\{\text{Re}^{\text{VI}}\text{NPh}\}]^{3-}$  and  $[\text{Bu}_4\text{N}][\text{PW}_{11}\text{O}_{39}\{\text{Re}^{\text{VI}}\text{NPh}\}]^{3-}$ . After irradiation, the recrystallization of the powder in acetonitrile under slow diffusion of diethyl ether gave crystals characterized by single X-ray diffraction by a cubic  $I$  cell ( $a = 17.661(3) \text{ \AA}$ ;  $V = 5509 \text{ \AA}^3$ ).

**Conclusion.** Nitrogenous derivatives of the Keggin polyanions were up to now restricted to nitrido<sup>11</sup> and nitrosyl derivatives.<sup>20</sup> We report here the first example of an organoimido derivative, and several characterization methods including electrochemistry and  $^1\text{H}$  and  $^{14}\text{N}$  NMR together with ESI mass spectrometry demonstrate without any ambiguity the formation of  $[\text{PW}_{11}\text{O}_{39}\{\text{Re}^{\text{V}}\text{NPh}\}]^{4-}$ . Mass spectrometry studies on polyoxometalates are steadily increasing and are of special interest for the insights they can give into the stability and reactivity of polyanions, in the gas phase.<sup>9e,25</sup> Work under current investigation also includes the use of other organoimido ligands either for an improvement of the synthesis of the Keggin derivatives or for the incorporation, on the aromatic ring, of a functional group.

**Acknowledgment.** The authors thank Dr. P. Gredin for recording the X-ray diffraction powder patterns and Dr. Carine Guyard-Duhayon for single-crystal X-ray diffraction experiments.

**Supporting Information Available:**  $^{31}\text{P}$  NMR spectra of  $[\text{Bu}_4\text{N}]_4[\text{PW}_{11}\text{O}_{39}\{\text{Re}^{\text{V}}\text{NPh}\}]$  and  $[\text{Bu}_4\text{N}]_4[\text{PW}_{11}\text{O}_{39}\{\text{Re}^{\text{V}}\text{O}\}]$  and indexation of X-ray diffraction powder diagrams. This material is available free of charge via the Internet at <http://pubs.acs.org>.

IC0499042

- (25) (a) Suslick, K. S.; Cook, J. C.; Rapko, B.; Droege, M. W.; Finke, R. G. *Inorg. Chem.* **1986**, *25*, 241. (b) Trovarelli, A.; Finke, R. G. *Inorg. Chem.* **1993**, *32*, 6034. (c) Lau, T. C.; Wang, J.; Guevremont, R.; Siu, K. W. M. *J. Chem. Soc., Chem. Commun.* **1995**, 877. (d) Deery, M. J.; Howarth, O. W.; Jennings, K. R. *J. Chem. Soc., Dalton Trans.* **1997**, 4783. (e) Truebenbach, C. S.; Howalla, M.; Hercules, D. M. *J. Mass Spectrom.* **2000**, *35*, 1121. (f) Waters, T.; J. O'Hair, R. A.; Wedd, A. G. *J. Am. Chem. Soc.* **2003**, *125*, 3384.